Molecular Cell *23*, 71–81, July 7, 2006 ©2006 Elsevier Inc. DOI 10.1016/j.molcel.2006.05.013

Structural Biology of RNA Polymerase III: Subcomplex C17/25 X-Ray Structure and 11 Subunit Enzyme Model

Anna J. Jasiak,[1,2] Karim-Jean Armache,[1,2] Birgit Martens,[1] Ralf-Peter Jansen,[1] and Patrick Cramer[1,*]
[1] Gene Center
Department of Chemistry and Biochemistry
Ludwig-Maximilians-University of Munich
Feodor-Lynen-Strasse 25
81377 Munich
Germany

Summary

We obtained an 11 subunit model of RNA polymerase (Pol) III by combining a homology model of the nine subunit core enzyme with a new X-ray structure of the subcomplex C17/25. Compared to Pol II, Pol III shows a conserved active center for RNA synthesis but a structurally different upstream face for specific initiation complex assembly during promoter selection. The Pol III upstream face includes a HRDC domain in subunit C17 that is translated by 35 Å and rotated by 150° compared to its Pol II counterpart. The HRDC domain is essential in vivo, folds independently in vitro, and, unlike other HRDC domains, shows no indication of nucleic acid binding. Thus, the HRDC domain is a functional module that could account for the role of C17 in Pol III promoter-specific initiation. During elongation, C17/25 may bind Pol III transcripts emerging from the adjacent exit pore, because the subcomplex binds to tRNA in vitro.

Introduction

RNA synthesis in the eukaryote nucleus is carried out by the multisubunit RNA polymerases I, II, and III. Whereas Pol I and Pol II synthesize ribosomal and mainly messenger RNA, respectively, Pol III transcribes small RNAs, including transfer RNAs, 5S ribosomal RNA, and U6 small nuclear RNA. Structural studies have so far concentrated on Pol II (reviewed in Armache et al. [2005a], Asturias [2004], Boeger et al. [2005], Cramer [2004], and Hahn [2004]). X-ray structures are known of the ten subunit Pol II core and its complexes (Bushnell et al., 2002, 2004; Cramer et al., 2000; Cramer et al., 2001; Gnatt et al., 2001; Westover et al., 2004a, 2004b) and of the complete 12 subunit Pol II and its complexes (Armache et al., 2003, 2005b; Bushnell and Kornberg, 2003; Kettenberger et al., 2003, 2004, 2006). Structural information on the other nuclear RNA polymerases is limited to electron microscopic investigations of Pol I (Bischler et al., 2002; Schultz et al., 1993).

Here, we report structural information on Pol III, the largest nuclear RNA polymerase (for reviews see Chedin et al. [1998a], Geiduschek and Kassavetis [2001], and Schramm and Hernandez [2002]). Pol III has a total molecular weight of around 0.7 MDa and comprises 17 subunits (Table 1). Nine Pol III subunits form a structural core (Table 1). The two largest subunits, C160 and C128, show substantial homology to the Pol II subunits Rpb1 and Rpb2, respectively. Five Pol III subunits are identical in Pol I and Pol II (Rpb5, Rpb6, Rpb8, Rpb10, and Rpb12). The Pol III subunits AC40 and AC19 are identical in Pol I and homologous to the Pol II subunits Rpb3 and Rpb11, respectively. On the periphery of the core enzyme, Pol III contains eight additional subunits, which form three distinct subcomplexes. The subcomplex C82/34/31 (Wang and Roeder, 1997; Werner et al., 1992) and the subcomplex C53/37/11 (Hu et al., 2002; Landrieux et al., 2006) are Pol III specific, although subunit C11 shows limited homology to the Pol II subunit Rpb9 and to the Pol II elongation factor TFIIS (Chedin et al., 1998b; Kettenberger et al., 2003). Finally, the Pol III subcomplex C17/25 has been suggested to be the counterpart of subcomplexes Rpb4/7 in Pol II (Hu et al., 2002; Sadhale and Woychik, 1994; Siaut et al., 2003), Rpa14/43 in Pol I (Meka et al., 2003; Peyroche et al., 2002; Shpakovski and Shematorova, 1999), and RpoF/E in archaeal RNA polymerase (Todone et al., 2001), although the corresponding subunit sequences show only weak conservation in some regions.

We present here the crystal structure and a functional analysis of the yeast Pol III subcomplex C17/25 and describe an 11 subunit model of Pol III. The results provide structural insights into Pol III and reveal specific features of the enzyme that can account for functional differences between nuclear RNA polymerases.

Results

Model of the Pol III Core

Based on the Pol II structure, we constructed a homology model for the Pol III nine subunit core. Subunits Rpb4, Rpb7, and Rpb9 were deleted from the Pol II structure (Armache et al., 2005b) because their homologies to potential Pol III counterparts were too weak. The common subunits Rpb5, Rpb6, Rpb8, Rpb10, and Rpb12 were retained in the model. For the Pol II subunits Rpb1, Rpb2, Rpb3, and Rpb11, sequence alignments with their Pol III homologs were obtained with CLUSTAL W (Thompson et al., 1994) and were used for an initial homology modeling. Side chains in these four Pol II subunits were kept when identical in the Pol III homologs and otherwise replaced by the most common rotamer of the counterpart residues. The resulting nine subunit model was inspected residue by residue. In most regions, the model showed meaningful internal nonpolar contacts and salt bridges, confirming the alignments. A few regions, however, showed steric clashes or disallowed contacts, indicating misalignment of the corresponding sequence stretches. Manual realignment of these weakly conserved stretches (Figure S1 available in the Supplemental Data with this article online) led to a model with good internal packing throughout. The three-dimensional context provided by the Pol II structure allowed for confirmation of the model, including

*Correspondence: cramer@lmb.uni-muenchen.de
[2] These authors contributed equally to this work.

Table 1. RNA Polymerase Subunits

Polymerase Part	Pol III Subunit	Pol II Subunit	Subunit Type	Sequence Identity (%)	Conserved Fold (%)
Core	C160	Rpb1	Homolog	28.4	83.2
	C128	Rpb2	Homolog	35.8	87.2
	AC40	Rpb3	Homolog	25.8	60.2
	AC19	Rpb11	Homolog	20.8	81.6
	Rpb5	Rpb5	Common	100	100
	Rpb6	Rpb6	Common	100	100
	Rpb8	Rpb8	Common	100	100
	Rpb10	Rpb10	Common	100	100
	Rpb12	Rpb12	Common	100	100
Rpb4/7 subcomplex	C17	Rpb4	Homolog	7.2	50
	C25	Rpb7	Homolog	25.2	81.3
Upstream subcomplex	C82/34/31		Specific	–	–
Downstream subcomplex	C53/37/11[a]	Rpb9[a]	Unclear	–	–
Eleven subunit Pol III model	–	–	–	39.4	83.4

[a] Subunit C11 shows homology to Rpb9 and TFIIS. Rpb9 was previously defined as a part of the Pol II core.

interactions that involve subunit interfaces and regions that are distant in the sequences.

X-Ray Analysis of the Pol III Subcomplex C17/25

The Pol II subcomplex Rpb4/7 could not be used in the Pol III modeling because of weak or apparently lacking sequence conservation with its Pol III counterpart C17/25. We therefore determined the C17/25 structure independently by X-ray crystallography (Experimental Procedures). After coexpression of C17 and C25 in *E. coli*, a soluble C17/25 heterodimer could be purified and crystallized. Because molecular replacement with the structures of Rpb4/7 (Armache et al., 2005b) and the archaeal counterpart RpoF/E (Todone et al., 2001) failed, the crystals were phased de novo with selenomethionine labeling and single anomalous diffraction (Table 2). The structure was refined at 3.2 Å resolution to a free R factor of 30.7% and showed good stereochemistry (Table 2).

Overall C17/25 Structure

The structure of C25 resembles that of its counterparts Rpb7 and RpoE (Figure 1). The N-terminal "tip" domain of C25 shows a root-mean-square deviation (rmsd) in Cα atom positions of 4.2 Å and 1.6 Å in Rpb7 and RpoE, respectively, whereas the C-terminal OB domain is quite divergent. The relative position of the two C25 domains differs slightly from that observed in Rpb7 (Figure S2). C25 differs from Rpb7 mainly by the absence of the short helical turn K* in the tip domain and the presence of a flexible, nonconserved loop, B4-B5, that is 34 residues longer than in Rpb7 (Figure 1).

The structure of C17 reveals a compact N-terminal "tip-associated" domain, which packs mainly against the C25 tip domain and not between the tip and OB domains as in Rpb4/7 and RpoF/E (Figure 1B). The only contact between the C17 tip-associated domain and the C25 OB domain is formed between C17 helix H2 and C25 loop B2-B3. Consistently, a mutation at the B2-B3 loop (S100P) impairs C17 binding in vivo (Zaros and Thuriaux, 2005). The C17 tip-associated domain connects via a flexible linker to a C-terminal HRDC domain, a fold that occurs in RecQ helicases and ribonucleases (Meka et al., 2003; Morozov et al., 1997). The C17 HRDC fold resembles the corresponding domains in Rpb4 and RpoF (rmsd in Cα positions of 2.07 and 4.5 Å, respectively, Figure S2), although the sequence conservation is very weak or absent (Figure 1A and Table 1).

The C17 HRDC Domain Adopts a Unique Position

Although the overall domain folds are conserved between C17/25 and Rpb4/7, the observed position of the C17 HRDC domain is very different from that in Rpb4 and RpoF (Figure 1B). Compared to Rpb4 or RpoF, the HRDC domain of C17 is translated by about 35 Å and rotated by about 150°. The C17 HRDC domain packs against the C25 OB domain, between the C2-C3 loop and the C terminus (Figures 1B and 2A). The HRDC-OB interface is complementary in shape and electrostatics (Figure 2A) and includes many hydrophobic residues, which are well conserved among several species (Figure S3) but are generally not conserved in the Pol I and Pol II counterparts (C25 residues F116, W130, M132, L138, and W211, and C17 residues M107, L121, and V124) (Figure 2B). Residues in the Rpb4 HRDC domain-Rpb7 interface are also conserved

Table 2. C17/25 X-Ray Diffraction Data and Refinement Statistics

Crystal	C17/25 SeMet	C17/25 Native
Data Collection[a]		
Space group	$P6_122$	$P6_122$
Wavelength (Å)	0.97932	0.97894
Unit cell axis (Å)	137.5, 240.6	138.2, 247.1
Resolution (Å)	50–3.5 (3.63–3.5)[b]	30–3.2 (3.31–3.2)
Completeness (%)	100	88.6 (91.4)
Unique reflections	17,684 (1,726)	21,061 (2,107)
Redundancy	14.4 (14.7)	3.9 (3.9)
R_{sym} (%)	10.3 (38.5)	9.1 (46.9)
$\langle I/\sigma I \rangle$	10.6 (8.3)	17.6 (2.6)
Refinement		
Amino acid residues		537
Rmsd bonds (Å)		0.007
Rmsd angles (°)		1.3
R_{cryst} (%)		23.6
R_{free} (%)		30.7

[a] Diffraction data were collected at beamline X06SA at the Swiss Light Source, Villigen, Switzerland.
[b] Numbers in parenthesis refer to the highest resolution shell.

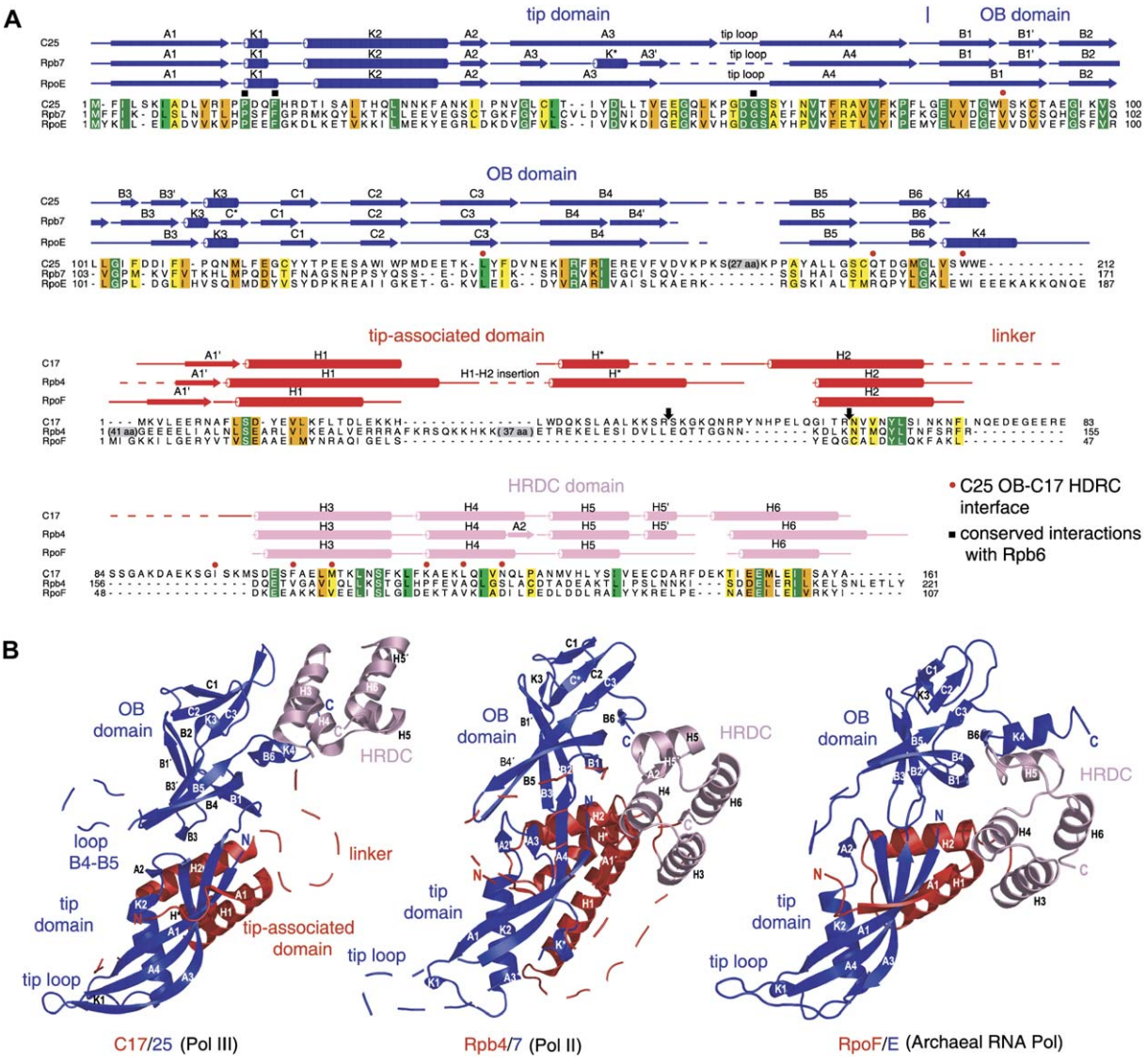

Figure 1. X-Ray Structure of the Pol III Subcomplex C17/25

(A) Primary and secondary structure. Structure-based alignments of amino acid sequences of *S. cerevisiae* C25 (top) and C17 (bottom) with their counterparts in Pol II (*S. cerevisiae* Rpb7 and Rpb4, respectively) and archaeal RNA polymerase (*M. jannaschii* RpoE and RpoF, respectively). Secondary structure elements are shown above the sequences (cylinders, α helices; arrows, β strands; lines, loops; and dashed lines, disordered). Conserved residues are highlighted according to decreasing conservation from green, through orange, to yellow. Cleavage sites revealed by limited proteolysis with trypsin are indicated with arrows. Three C25 residues involved in conserved interactions with Rpb6 are indicated with a black square. Residues that contribute to the C25-C17 HRDC interface are indicated with a red dot.

(B) Comparison of the structures of yeast C17/25 (this study, left) with that of yeast Rpb4/7 (Armache et al., 2005b) (center) and archaeal RpoF/E (Todone et al., 2001) (right). C25/Rpb7/RpoE are in blue and C17/Rpb4/RpoF are in red, with the HRDC domain in light red. Disordered in the C17/25 structure are the C25 loop B4-B5 (residues K59–K90), the C17 loop H*-H2 (residues K38–N47), and the C17 linker between the tip-associated domain and the HRDC domain (residues N69–G94). Figures were prepared with PYMOL (DeLano Scientific).

among *S. cerevisiae*, *S. pombe*, and human, but not in C17/25. Thus, the C17 HRDC-C25 interface is unique and Pol III specific, suggesting that the observed position of the HRDC domain is a specific feature of Pol III. The same position of the C17 HRDC domain may in principle be adopted in other species. Although, in the human and *S. pombe* sequences, the C17 linker is apparently only three residues long, the distance between the two C17 domains could just be spanned if the residues corresponding to C17 residues 95–100 adopt an extended conformation.

Modular Two-Domain Structure of C17

Although the well-packed nature of the HRDC-OB interface suggests that the location of the HRDC domain is fixed, there is evidence that the domain can change its position. First, the asymmetric unit of the crystals contains two C17/25 heterodimers, but only one HRDC domain is ordered, whereas the second one is not visible in the electron density, consistent with a low affinity of the HRDC-OB interface. Second, the linker between the C17 tip-associated domain and the HRDC domain is flexible and not conserved among species (Figure S3). To test if

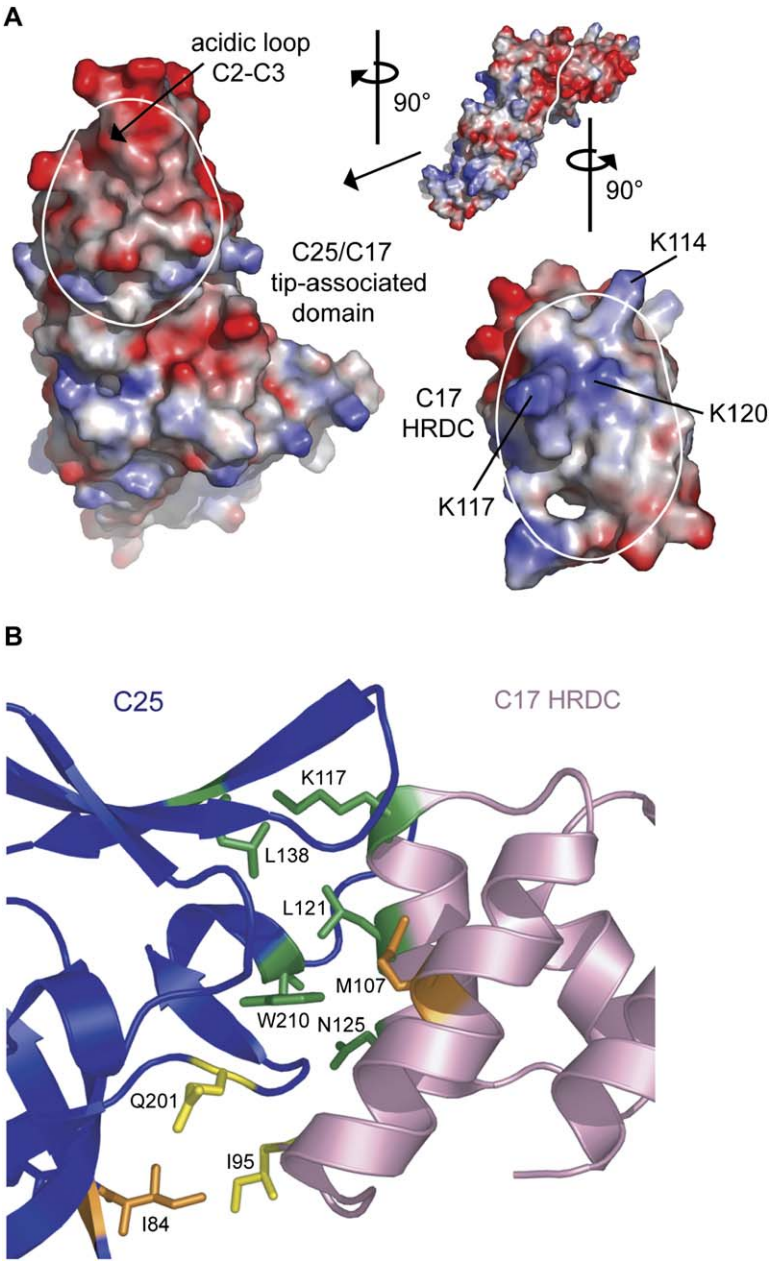

Figure 2. Interface between C25 OB Domain and the C17 HRDC Domain

(A) Electrostatic surfaces. In the center, a surface representation of C17/25 is shown colored according to the electrostatic surface potential (positive, blue; negative, red). The view is as in Figure 1B. A book view of the interface was obtained by separating the C17 HRDC domain from the complex. The remainder of C17/25 and the C17 HRDC domain are depicted to the left and to the right, respectively.

(B) Detailed view of the interface. Residues are highlighted according to decreasing conservation among species from green, through orange, to yellow (compare Figure S3). The view is very similar to that in Figure 1B.

the C17 HRDC domain forms an independently folding module, we expressed the isolated domain in *E. coli* (Experimental Procedures). Size exclusion chromatography and static light scattering revealed that the purified soluble C17 HRDC domain is stable at room temperature for at least one week (8.59/8.75 kDa observed/theoretical molecular weight, data not shown). Together these results show that C17/25 is a modular subcomplex and that the C17 HRDC domain is an autonomously folding module, which may adopt different positions.

Both C17 Domains Are Essential In Vivo

In contrast to Rpb4, C17 is essential for viability of *S. cerevisiae*. To investigate if the essential in vivo function requires both structural domains of C17, we generated plasmids under the control of the heterologous *GAL1* promoter that carried the gene for full-length C17 (*RPC17*), an *RPC17* mutant lacking the HRDC domain (*RPC17*ΔHRDC), or the HRDC domain alone. Plasmids were introduced into an *rpc17*Δ yeast strain that was rescued by *RPC17* on a centromeric *URA3* plasmid. Loss of the *URA3* plasmid due to complementation by any of the *GAL1* promoter-driven expression constructs would allow growth on media containing 5′-fluorotic acid (5′-FOA). In these experiments, complementation was allowed by full-length *RPC17*, but not by *RPC17*ΔHRDC or by the HRDC domain alone (Figure 3). The same result was obtained at 30ºC and 23ºC. Thus, both C17 domains are required for cell viability, and the HRDC domain has an essential function in vivo that requires its proximity to the C17/25 subcomplex.

In an attempt to test if the essential in vivo function of the HRDC domain requires its positioning as observed in the crystal structure, we mutated the *RPC17* plasmid

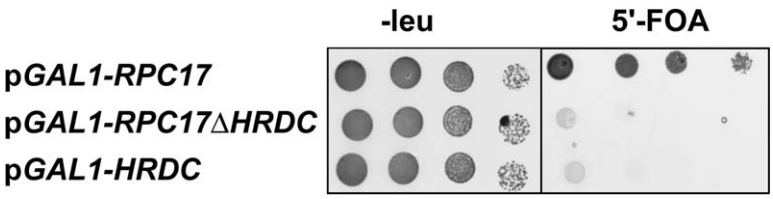

Figure 3. The C17 HRDC Domain Is Essential for Cell Viability

A yeast strain carrying an *rpc17* deletion and *RPC17* on a centromeric *URA3* plasmid was transformed with centromeric *LEU2* plasmids containing *RPC17*, an *RPC17*ΔHRDC, or the isolated C17 HRDC domain under control of the heterologous *GAL1* promoter. Left, serial dilutions of each strain grown on −leu plates. Right, serial dilutions of each strain grown on plates containing 5′-FOA. Only full-length *GAL1-RPC17* can complement for the loss of the *URA3* plasmid carrying wild-type *RPC17* and thus allows growth on 5′-FOA.

such that the hydrophobic residues F103 and M107, both located in the interface between the C17 HRDC domain and the C25 OB domain, were changed to glutamates. The resulting C17 double mutant F103E/M107E is predicted to disrupt the domain interface but did still support cell growth at either 30ºC or 23ºC (data not shown). This supports a possible mobility of the HRDC domain and suggests that the position of the domain in a functional in vivo complex could differ from that observed in the C17/25 crystal structure. It remains, however, possible that the mutated HRDC domain is retained in the observed position in the context of the complete Pol III enzyme by interactions with additional Pol III subunits.

C17/25 Binds Nucleic Acids In Vitro

To explore possible functions of C17/25, we subjected the purified recombinant subcomplex to nucleic acid binding assays (Experimental Procedures). We performed nonradioactive electrophoretic mobility shift assays (EMSAs) and revealed the nucleic acids by staining with SYBR-Gold (Molecular Probes). Similar to Rpb4/7 and Rpa14/43 (Meka et al., 2003, 2005; Orlicky et al., 2001), C17/25 bound to single-stranded RNA (Figure 4A). Comparative EMSA analysis showed that C17/25 bound much stronger to a tRNA sample, with an apparent affinity in the low micromolar range (Figure 4B). Binding to duplex DNA was also observed but was weaker than for tRNA (Figure 4C). Single-stranded DNA binding to C17/25 was very weak (data not shown). All these nucleic acid probes were also bound by recombinant purified Rpb4/7 but generally less efficiently than by C17/25 (Figure 4, and data not shown). In particular, Rpb4/7 bound more weakly to tRNA, although it also shows a preference for tRNA relative to the 22 nt ssRNA (Figure 4B). There was generally no indication of sequence specificity in nucleic acid binding. On the longer nucleic acid probes, multiple shifted bands are observed that could correspond to multiple complexes, complicating the interpretation of the results.

To check whether the C17 HRDC domain is responsible for the nucleic acid binding property of C17/25, we performed EMSA with the isolated HRDC domain. The purified HRDC domain did not show detectable nucleic acid binding, even when a 100-fold or greater excess of the protein over nucleic acids was used (Figure 4). Indeed, the HRDC domain surface contains only one small cluster of positively charged residues (lysines K114, K117, and K120) that is involved in interaction with the C25 acidic loop C2-C3 (residues D133, E134, and

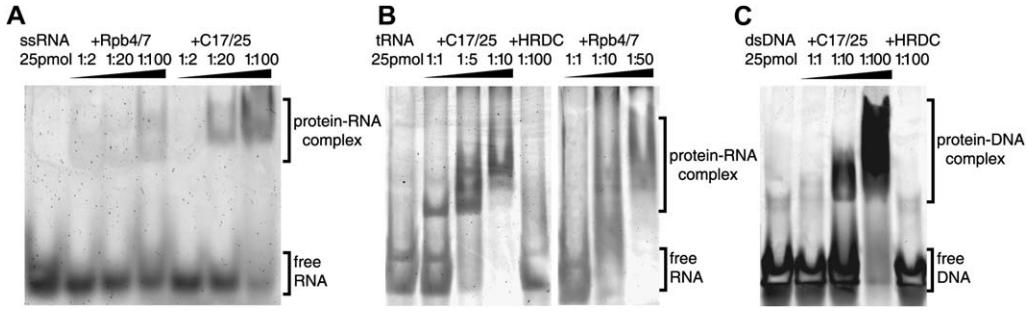

Figure 4. Nucleic Acid Binding Properties of C17/25, the C17 HRDC Domain, and Rpb4/7

(A) Comparison of the single-stranded RNA binding activity of the subcomplexes Rpb4/7 and C17/25. Increasing amounts of the proteins were incubated with 25 pmol of a 22-mer single-stranded RNA and the resulting complexes separated from free RNA by electrophoresis. EMSAs were carried out as described in the Experimental Procedures. Nucleic acids were revealed by SYBR-Gold staining.

(B) C17/25 binds tRNA. Increasing amounts of C17/25 were incubated with 25 pmol of a commercial tRNA preparation from *E. coli* (Sigma), and the resulting complexes were separated from free tRNA by electrophoresis. A significant bandshift was observed already when the ratio of tRNA to C17/25 complex was 1:1, indicating a dissociation constant in the low micromolar range. A complete shift of the nucleic acids was observed at a 10-fold excess of C17/25 over tRNA, whereas a 50-fold excess of Rpb4/7 was required to obtain the same effect. The free C17 HRDC domain does not show significant tRNA binding even at a 100-fold excess of protein over tRNA. The double bands visible in free and bound tRNA samples may be due to conformational heterogeneity of the tRNA sample.

(C) C17/25 binds duplex DNA. Increasing amounts of C17/25 were incubated with 25 pmol of a 40 base pair duplex DNA, and the resulting complexes were separated from free DNA by electrophoresis. A significant bandshift was observed only when an excess of protein was used. The free C17 HRDC domain does not show significant DNA binding even at a 100-fold excess of protein.

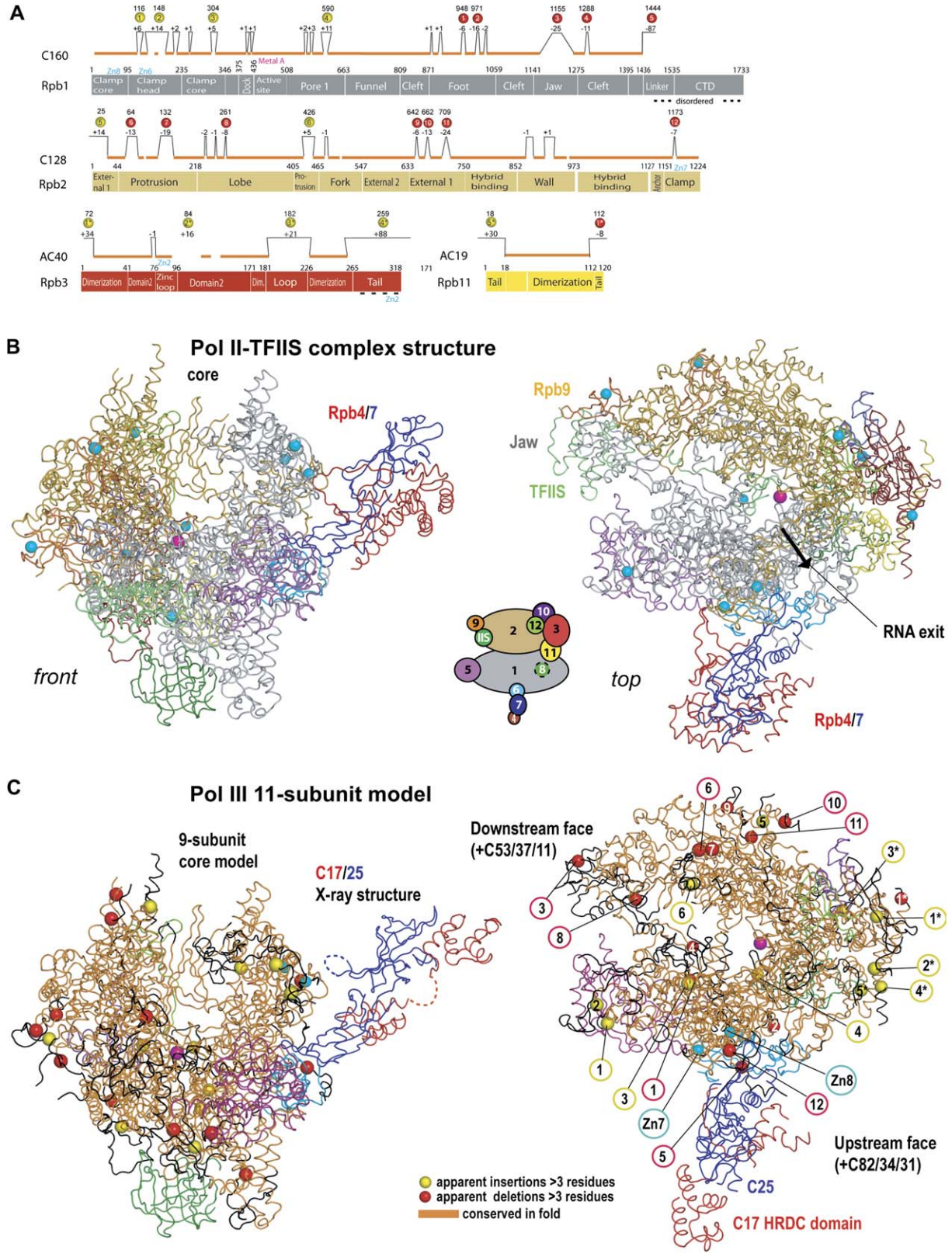

Figure 5. Eleven Subunit Pol III Model

(A) Pol II structure-guided sequence alignments of core subunits homologous in Pol III. The domain organization of Pol II subunits Rpb1, Rpb2, Rpb3, and Rpb11 is shown as diagrams (Cramer et al., 2001). Above the diagrams, regions conserved in fold in the homologous subunits of Pol III are indicated with orange bars. Regions that apparently adopt a different structure are indicated with black brackets. Indicated are the numbers of residues apparently inserted or deleted in the Pol III subunits (depicted only for more than three residues inserted or deleted). The numbers correspond to the Pol II residue N-terminal (at the beginning) of the insertion/deletion in Pol III. For detailed alignments see Figure S1.

E135) (Figure 2A). In conclusion, there is no evidence for a nucleic acid binding function of the C17 HRDC domain, but our observations cannot exclude that nucleic acid interactions account for the essential in vivo function of the domain.

Interaction of C17/25 with Core Pol III

In the Pol II structure, the Rpb4/7 subcomplex binds the Pol II core via two loops in its Rpb7 tip domain: the "tip loop" and the A1-K2 loop (Armache et al., 2003, 2005b; Bushnell and Kornberg, 2003). The two corresponding loops in C17/25 are ordered in one copy of the asymmetric unit of our crystals and adopt a similar conformation as in Pol II. We superimposed the two core binding loops of C25 with those of Rpb7 to place the C17/25 structure onto the Pol III core model. The resulting C25 tip-core Pol III interface reveals that key contacts with the common core subunit Rpb6 are formed by C25 residues P15, F18, and G64, which are conserved in Rpb7 (Figure 1A), indicating that the placement of C17/25 is correct. The specificity in the interaction between C17/25 and the Pol III core may arise at least partially from a salt bridge between glutamate E56 in C25 and lysine K1432 in C160, which corresponds to isoleucine I1445 in Rpb1 (data not shown).

Eleven Subunit Pol III Model

The correct docking of the C17/25 X-ray structure onto the homology model of the Pol III core resulted in a model for the 11 subunit central part of Pol III, which lacks only the subcomplexes C82/34/31 and C53/37/11 (Figure 5). Due to the C17 HRDC domain, which adopts a new position, and due to the slightly different relative orientation of the C25 tip and OB domains, the model shows an orientation of C17/25 relative to the core Pol III that differs from that of Rpb4/7 in Pol II (Figure 5). Compared to Rpb4/7, C17/25 protrudes from the Pol III core more toward the upstream face and RNA exit pore (Figure 5). The exact orientation of C17/25, however, may differ in the complete Pol III, due to the presence of the two additional subcomplexes or due to some remodeling in the interface between the C25 tip and core Pol III.

Discussion

Structural Biology of Pol III

Here, we present structural information on Pol III. A homology model of the nine subunit Pol III core was obtained with the Pol II structure. The X-ray structure of the Pol III subcomplex C17/25 and biochemical data revealed that the C17 HRDC domain forms an independently folded module that adopts an unexpected new position and may be mobile. Complementation analysis in yeast demonstrated an essential function of the C17 HRDC domain in vivo. EMSA analysis revealed that C17/25 binds various types of nucleic acids in vitro, including tRNA, but that this activity does not reside in the C17 HRDC domain. Combination of the C17/25 structure with the Pol III core model resulted in an 11 subunit model for Pol III that allows interpretation of biochemical and genetic data and the design of mechanistic studies of Pol III transcription.

Polymerase Conservation and Elongation

Our results reveal that at least 83.4% of the Pol II fold is conserved in Pol III, although the overall sequence identity is only 39.4% (Table 1). The only Pol II domain folds that are not present or strongly altered in Pol III are the Rpb1 jaw domain and the Rpb2 external domain 1 (Cramer et al., 2001) (Figure 5). Other differences concern only insertions and deletions on the enzyme surface (Figure 5). Comparison with the Pol II elongation complex structures (Gnatt et al., 2001; Kettenberger et al., 2004; Westover et al., 2004a) shows that extended surfaces conserved between Pol III and Pol II are only found in the polymerase cleft, around the incoming DNA, in the active site, around the binding sites for the nucleoside triphosphate substrate and the DNA-RNA hybrid, and at the RNA exit tunnel (Figure 6, and data not shown), reflecting the conservation of the basic mechanisms of RNA elongation in the two polymerases.

RNA Binding of Rpb4/7-like Subcomplexes

The functional conservation of RNA polymerases may extend to binding of the exiting RNA to the Rpb4/7-like subcomplexes, which are located in proximity of the RNA exit pore. Indeed, RNA emerging from a Pol II elongation complex can be crosslinked to Rpb7 (Ujvari and Luse, 2006). Further, Rpb4/7, A14/43, and RpoE/F all bind single-stranded nucleic acids (Meka et al., 2003, 2005; Orlicky et al., 2001). We show that C17/25 also binds single-stranded RNA, suggesting that interaction with exiting RNA is a common property of all Rpb4/7-like complexes. C17/25 bound most strongly to tRNA, suggesting that it may preferentially interact with Pol III transcripts that emerge from the RNA exit pore located in the vicinity of the subcomplex (shown for Pol II as a black arrow in Figure 5B). Consistently, Rpb4/7 bound more weakly to tRNA, and the surfaces of the two subcomplexes are not conserved, including a RNA binding patch of Rpb4/7 (Meka et al., 2005). It is thus possible that emerging Pol III transcripts fold cotranscriptionally on the C17/25 surface or that C17/25 plays a role in coupling Pol III transcription and RNA processing. However, more experiments must be conducted to rigorously address the possibility of preferential interaction of C17/25 with various Pol III transcripts.

Promoter-Specific Initiation and the Upstream Subcomplex C82/34/31

Pol III selects its promoters with specific transcription initiation factors that assemble on the enzyme upstream

(B) Structure of the complete Pol II-TFIIS complex (Kettenberger et al., 2003, 2004). The Pol II subunits Rpb1-Rpb12 and TFIIS are colored according to the key. Eight zinc ions and the active site magnesium ion are depicted as cyan spheres and a pink sphere, respectively.
(C) Model of an 11 subunit form of Pol III. The model was obtained by combining the nine subunit homology model of the Pol III core with the X-ray structure of the C17/25 complex. Regions in homologous subunits that are conserved in fold are in orange according to (A). Black regions are not present or altered in Pol III. Deletions and insertions in Pol III amino acid sequences as compared with Pol II are shown as red and yellow spheres, respectively, if they exceed three amino acid residues in length (A). The two Pol III subcomplexes C82/34/31 and C53/37/11, which are missing from the model, are predicted to locate to the upstream and downstream face, respectively.

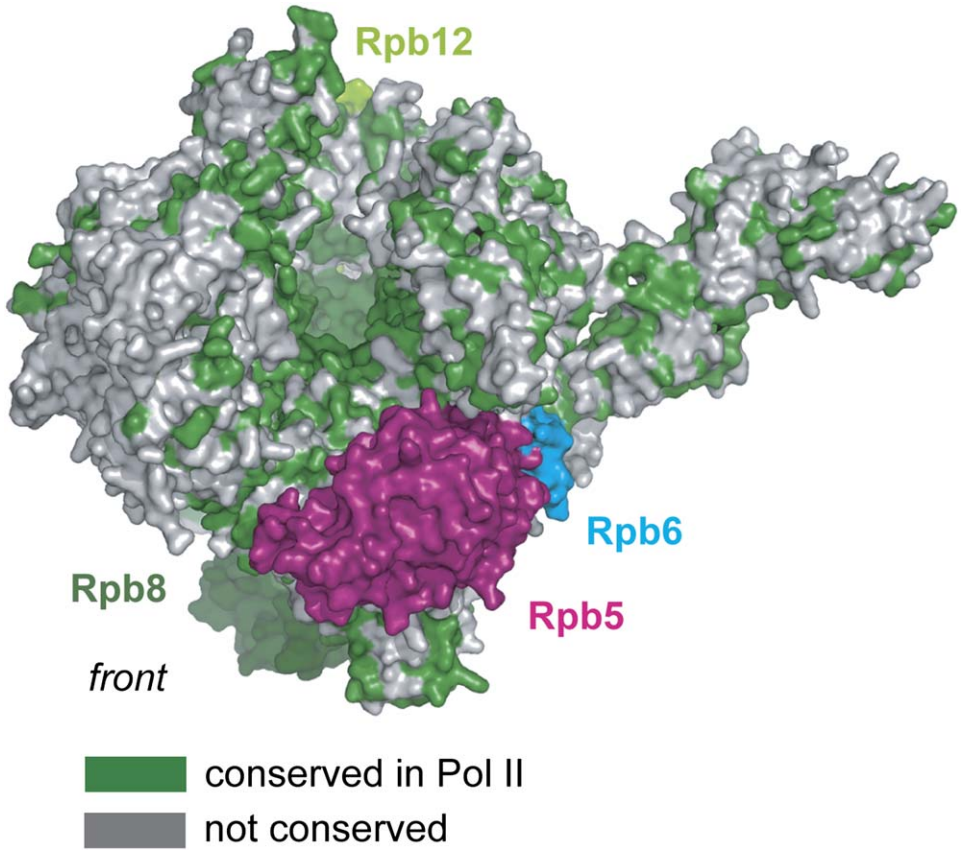

Figure 6. Surfaces on the Pol III Model Conserved in Pol II

Residues on the surface of the 11 subunit Pol III model of Figure 5C that are identical or conserved in the four homologous subunits of *S. cerevisiae* Pol II are in green, others are in silver. The common subunits are in different colors. Extensive conservation is observed only in the active center cleft.

face. The Pol III upstream face is structurally different from that of Pol II and includes C17/25 with its differently positioned HRDC domain. The functional importance of C17/25 for initiation is established by a point mutation in C25 that results in an initiation defect (Zaros and Thuriaux, 2005). Indeed, C17/25 contributes to initiation complex assembly, because C17 binds to the Pol III initiation factor TFIIIB (Ferri et al., 2000) and to the Pol III subcomplex C82/34/31 (Figure 5) (Geiduschek and Kassavetis [2001]; Schramm and Hernandez [2002], and references therein). The C82/34/31 subcomplex also binds the Pol III core near a zinc site (Werner et al., 1992) (Zn8 in Figure 5C), where the Pol III subunit C128 shows a specific seven residue deletion (Figure 5C, deletion 12). C82/34/31 bridges to the initiation factors TFIIIC (Hsieh et al., 1999) and TFIIIB (Geiduschek and Kassavetis [2001], Schramm and Hernandez [2002], and references therein). Because C17 is part of an extensive protein interaction network, and because the C17 HRDC domain has an essential in vivo function but apparently lacks nucleic acid binding activity, the HRDC domain is most likely involved in Pol III initiation complex assembly. C17/25 could, however, also contribute directly to promoter binding because it has an affinity for duplex DNA. In this respect, it is interesting that Rpb4/7 can be crosslinked to promoter DNA in a Pol II initiation complex (Chen et al., 2004).

The Downstream Subcomplex C53/37/11 and Termination

Termination of Pol III transcription is triggered by a stretch of thymine residues in the DNA template (Cozzarelli et al., 1983), whereas Pol II requires additional polypeptides for termination. Pol III termination depends on the C53/37/11 subcomplex (Landrieux et al., 2006). This subcomplex apparently occupies a downstream location, near the site of DNA entry into the polymerase cleft and at the polymerase funnel and pore, because subunit C11 consists of zinc binding N- and C-terminal domains that were suggested to correspond to the N-terminal domain of Rpb9 and the C-terminal domain of TFIIS, respectively (Figure 5). An equivalence of the C-terminal domains of C11 and TFIIS is suggested by their shared function in RNA cleavage stimulation and by a shared functionally essential residue (Chedin et al., 1998b; Kettenberger et al., 2003). C11, and in particular its N-terminal domain, cannot be modeled, however, because the Rpb1 jaw domain, which binds Rpb9, is absent or strongly altered in Pol III (Figure 5 and Figure S1). It remains unclear how the structural differences on the downstream face of Pol III and Pol II can account for the different termination mechanisms.

Specific Polymerase Assembly

Comparison of the subunit interfaces in Pol III and Pol II suggests the basis for specific enzyme assembly. The

AC40-AC19 heterodimer is specifically formed with hydrophobic interface residues that differ in size in the corresponding Rpb3-Rpb11 dimer (in particular, L33 in Rpb3 and A48 in Rpb11 are replaced by F67 and Y78, respectively, in AC40 and AC19). The interaction of AC40/19 with the Pol III subunit C128 involves three invariant interface residues (C128 residues Y765, F933, and Y1005, corresponding to Rpb2 residues Y833, F1001, and Y1073, respectively) and may be specific due to a salt bridge between glutamate E1011 in C128 (K1079 in Rpb2) and arginine R295 in AC40 (A225 in Rpb3) in the model. Specific interaction between the two large subunits is difficult to rationalize because they form an extended interface. The common subunits can bind at equivalent locations on the surface of Pol III and Pol II, because key interface residues are identical in the homologous subunits of the polymerases. For example, a hydrophobic pocket of Rpb5 embeds an invariant phenylalanine from the largest polymerase subunit (F914 in C160, F866 in Rpb1), but the interfaces of Rpb5 with the largest subunit of the enzymes are otherwise divergent. In Rpb12, two basic residues form salt bridges with two invariant acidic residues in the second largest subunit (Rpb2 residues E116 and D896, C128 residues E117 and D827). A complete list of these invariant residues in homologous polymerase subunits that form conserved contacts with the common polymerase subunits is given in Table S1. Because these contacts are also present in Pol I, the common subunits are found on equivalent positions on all three nuclear RNA polymerases.

Conclusions

Pol III is a key enzyme for the expression of the eukaryote genome but so far has resisted structural investigation. Here, we used a combination of X-ray crystallography, molecular modeling, and functional in vitro and in vivo analysis to establish an 11 subunit model of Pol III and to provide molecular insights into similarities and differences with Pol II. Whereas the similarity of the core fold and active center of Pol III and Pol II reflects a common basic transcription mechanism, structural differences in a region that directs initiation complex assembly partially account for promoter specificity. Our data provide a framework for further structural and functional analysis of Pol III and mark the beginning of a comparative molecular analysis of eukaryotic RNA polymerases.

Experimental Procedures

Sample Preparations

The genes for C17 and C25 were amplified from yeast genomic DNA by PCR and were cloned into vector pET21b (Novagen) as described (Sakurai et al., 1999), resulting in a C-terminal hexahistidine tag (His) on C25. C17/25 was expressed for 15 hr at 18ºC in *E. coli* BL21(DE3)RIL cells (Stratagene). Cells were harvested by centrifugation, resuspended in buffer A (1 M NaCl, 50 mM Tris [pH 8.0], 5% glycerol, and 10 mM β-mercaptoethanol) and were lysed by sonication. After centrifugation, the supernatant was loaded onto a Ni-NTA column (Qiagen) equilibrated with buffer A. The column was washed stepwise with 10 ml of buffer A and 5 ml of buffer A containing 20 mM imidazole. Proteins were eluted with buffer A containing 150 mM imidazole. Eluted fractions were diluted 6.5-fold with buffer B (50 mM Tris [pH 8.0], 1 mM EDTA, and 5 mM DTT) and further purified by anion exchange chromatography (MonoQ, Amersham). The column was equilibrated with buffer C (150 mM NaCl, 50 mM Tris [pH 8.0], 1 mM EDTA, and 5 mM DTT), and proteins were eluted with a linear gradient of ten column volumes from 150 mM to 1 M NaCl. After concentration, the sample was applied to a Superose-12 HR gel filtration column (Amersham) equilibrated with buffer D (40 mM ammonium sulfate, 10 μM $ZnCl_2$, 5 mM HEPES [pH 8.5], and 10 mM DTT). Pooled peak fractions were concentrated for crystallization to 8.5 mg/mL. To subclone the C17 HRDC domain, the region of the gene corresponding to amino acid residues 94–161 was amplified by PCR from the C17/25 expression plasmid and cloned into pET21b (Novagene) with a C-terminal His tag. Expression and purification of the HRDC domain were essentially as for C17/25, except that buffer A contained 150 mM NaCl. The purified HRDC domain was concentrated to 10 mg/mL, flash frozen in liquid nitrogen, and stored in −80ºC.

C17/25 Crystal Structure Determination

Crystals of native C17/25 subcomplex were grown at 20ºC with the hanging-drop method, using as reservoir solution 3% PEG400, 0.1 M HEPES (pH 7.5), 1.6 M ammonium sulfate, and 0.1 M NaCl. The crystals reached a maximum size of 350 μm × 140 μm × 140 μm. For SAD phasing, selenomethionine-containing C17/25 was prepared as described (Budisa et al., 1995; Meinhart et al., 2003) and was crystallized as above, except that 0.15 M NaCl was used in the reservoir solution. Crystals were harvested in reservoir solution additionally containing 5% glycerol. The glycerol concentration was increased to 30% in four steps, using an incubation time of 2 min per step. The crystals were flash-cooled by plunging into liquid nitrogen. The SAD experiment on selenomethionine-labeled crystals and native crystal measurements were performed at the Swiss Light Source (Table 2). Data were processed with DENZO and SCALEPACK (Otwinowski and Minor, 1996). The program SnB (Weeks and Miller, 1999) detected 12 selenium sites, which were used as seeds in program SOLVE (Terwilliger, 2002). This resulted in a total of 18 selenium peaks that stemmed from two C17/25 complexes in the asymmetric unit. After SAD phasing with all sites in SOLVE, program RESOLVE was used for density modification and NCS averaging and was able to autobuild an initial model, which was corrected and completed manually with program O (Jones et al., 1991). Because native crystals showed slightly different unit cell dimensions, the resulting model was used for molecular replacement with program PHASER (McCoy et al., 2005). The C17/25 model was subsequently refined against native data at 3.2 Å resolution to a free R factor of 30.7% (Table 2). In the refined structure, 99% of the residues fall in allowed and additionally allowed regions of the Ramachandran plot, and none of the residues are in disallowed regions.

EMSAs

Nucleic acid probes included single-stranded DNA and RNA 22-mers (ssRNA, 5′-UAUAUGCAUAAAGACCAGGC-3′; ssDNA, 5′-ATG AAAGTTCTTGAGGAAAGG-3′), a double-stranded 40 base pair DNA (5′-ACCGAAAGCTTTATATAGGCTATTGCCCAAAAATGTATCG CCAATCACCTAATTTGGAG-3′), obtained by annealing complementary synthetic single strands, and an *E. coli* tRNA preparation (Sigma). Twenty-five picomoles of tRNA, duplex DNA or ssRNA, or 50 pmol of ssDNA was incubated with different amounts of protein in 20 μl of binding buffer for 30 min on ice as described (Orlicky et al., 2001). Bound and free probes were resolved by electrophoresis in native 4%–20% acrylamide TBE gradient gels (Invitrogen) (or in 7.5% polyacrylamide 0.5 × TBE gels containing 2% glycerol, in case of single-stranded nucleic acids) at 100 V for 2.5 hr at 4ºC. Gels were stained for 30 min with SYBR-Gold (Molecular Probes) and visualized on a Typhoon 9400 phosphoimager (Amersham). Afterward, the gels were restained with Coomassie Brilliant Blue R (Roth) solution to localize the protein bands. This ensured colocalization of nucleo-protein complexes (data not shown).

Yeast Complementation Studies

Diploid *S. cerevisiae* strain Y26779 containing a heterozygous deletion of the C17 gene, *RPC17* (Euroscarf, Frankfurt, Germany), was transformed with plasmid RJP1207 (p416-*URA3*- p*GAL1-RPC17*) and sporulated. Haploid cells were selected carrying the *rpC17Δ::kan*^{R} deletion and the complementing plasmid. The resulting strain

(RJY2771) was transformed with plasmid RJP1208 (p415-*LEU2*-p*GAL1-RPC17*), RJP1209 (p415-*LEU2*- p*GAL1-rpC17ΔHRDC*), or RJP1210 (p415-*LEU2*- p*GAL1-HRDC*), generated by cloning into vector p415-*LEU2*-p*GAL1* BamHI-XhoI fragments of the complete PCR-amplified ORF of *RPC17*, the N-terminal 80 amino acids of *RPC17*, or its C-terminal 68 residue HRDC domain, respectively. Start and stop codons were introduced by PCR mutagenesis. The double mutation F103E/M107E of C17 was introduced into plasmid p415-*LEU2*- p*GAL1-RPC17* with the use of the QuikChange kit (Stratagene). Transformed yeast strains were selected on −leu plates containing 2% galactose to induce expression of the corresponding construct. Single clones were resuspended and spotted in serial dilutions on plates containing 5′-FOA to test for loss of plasmid RJP1207, indicating complementation by the corresponding construct.

Supplemental Data

Supplemental Data include three figures and one table and can be found with this article online at http://www.molecule.org/cgi/content/full/23/1/71/DC1/.

Acknowledgments

We thank M. Bertero, S. Lange, L. Lariviere, S. Mitterweger, and K. Sträßer (Gene Center Munich) for help. This work was supported by the Deutsche Forschungsgemeinschaft, the Sonderforschungsbereich SFB646 "Regulatory networks in genome expression and maintenance," the Doktorandenkolleg "NanoBioTech" within the Elitenetzwerk Bayern, and the Fonds der chemischen Industrie. Part of this work was perfomed at the Swiss Light Source (SLS) at the Paul Scherrer Institut, Villigen, Switzerland. We thank C. Schulze-Briese and his team for help at the SLS.

Received: March 7, 2006
Revised: April 27, 2006
Accepted: May 8, 2006
Published: July 6, 2006

References

Armache, K.-J., Kettenberger, H., and Cramer, P. (2003). Architecture of the initiation-competent 12-subunit RNA polymerase II. Proc. Natl. Acad. Sci. USA *100*, 6964–6968.

Armache, K.-J., Kettenberger, H., and Cramer, P. (2005a). The dynamic machinery of mRNA elongation. Curr. Opin. Struct. Biol. *15*, 197–203.

Armache, K.-J., Mitterweger, S., Meinhart, A., and Cramer, P. (2005b). Structures of complete RNA polymerase II and its subcomplex Rpb4/7. J. Biol. Chem. *280*, 7131–7134.

Asturias, F.J. (2004). RNA polymerase II structure, and organization of the preinitiation complex. Curr. Opin. Struct. Biol. *14*, 121–129.

Bischler, N., Brino, L., Carles, C., Riva, M., Tschochner, H., Mallouh, V., and Schultz, P. (2002). Localization of the yeast RNA polymerase I-specific subunits. EMBO J. *21*, 4136–4144.

Boeger, H., Bushnell, D.A., Davis, R., Griesenbeck, J., Lorch, Y., Strattan, J.S., Westover, K.D., and Kornberg, R.D. (2005). Structural basis of eukaryotic gene transcription. FEBS Lett. *579*, 899–903.

Budisa, N., Steipe, B., Demange, P., Eckerskorn, C., Kellermann, J., and Huber, R. (1995). High-level biosynthetic substitution of methionine in proteins by its analogs 2-aminohexanoic acid, selenomethionine, telluromethionine and ethionine in Escherichia coli. Eur. J. Biochem. *230*, 788–796.

Bushnell, D.A., and Kornberg, R.D. (2003). Complete RNA polymerase II at 4.1 Å resolution: implications for the initiation of transcription. Proc. Natl. Acad. Sci. USA *100*, 6969–6972.

Bushnell, D.A., Cramer, P., and Kornberg, R.D. (2002). Structural basis of transcription: alpha-amanitin-RNA polymerase II cocrystal at 2.8 A resolution. Proc. Natl. Acad. Sci. USA *99*, 1218–1222.

Bushnell, D.A., Westover, K.D., Davis, R.E., and Kornberg, R.D. (2004). Structural basis of transcription: an RNA polymerase II-TFIIB cocrystal at 4.5 Angstroms. Science *303*, 983–988.

Chedin, S., Ferri, M.L., Peyroche, G., Andrau, J.C., Jourdain, S., Lefebvre, O., Werner, M., Carles, C., and Sentenac, A. (1998a). The yeast RNA polymerase III transcription machinery: a paradigm for eukaryotic gene activation. Cold Spring Harb. Symp. Quant. Biol. *63*, 381–389.

Chedin, S., Riva, M., Schultz, P., Sentenac, A., and Carles, C. (1998b). The RNA cleavage activity of RNA polymerase III is mediated by an essential TFIIS-like subunit and is important for transcription termination. Genes Dev. *12*, 3857–3871.

Chen, B.S., Mandal, S.S., and Hampsey, M. (2004). High-resolution protein-DNA contacts for the yeast RNA polymerase II general transcription machinery. Biochemistry *43*, 12741–12749.

Cozzarelli, N.R., Gerrard, S.P., Schlissel, M., Brown, D.D., and Bogenhagen, D.F. (1983). Purified RNA polymerase III accurately and efficiently terminates transcription of 5S RNA genes. Cell *34*, 829–835.

Cramer, P. (2004). Structure and function of RNA polymerase II. Adv. Protein Chem. *67*, 1–42.

Cramer, P., Bushnell, D.A., Fu, J., Gnatt, A.L., Maier-Davis, B., Thompson, N.E., Burgess, R.R., Edwards, A.M., David, P.R., and Kornberg, R.D. (2000). Architecture of RNA polymerase II and implications for the transcription mechanism. Science *288*, 640–649.

Cramer, P., Bushnell, D.A., and Kornberg, R.D. (2001). Structural basis of transcription: RNA polymerase II at 2.8 angstrom resolution. Science *292*, 1863–1876.

Ferri, M.L., Peyroche, G., Siaut, M., Lefebvre, O., Carles, C., Conesa, C., and Sentenac, A. (2000). A novel subunit of yeast RNA polymerase III interacts with the TFIIB-related domain of TFIIIB70. Mol. Cell. Biol. *20*, 488–495.

Geiduschek, E.P., and Kassavetis, G.A. (2001). The RNA polymerase III transcription apparatus. J. Mol. Biol. *310*, 1–26.

Gnatt, A.L., Cramer, P., Fu, J., Bushnell, D.A., and Kornberg, R.D. (2001). Structural basis of transcription: an RNA polymerase II elongation complex at 3.3 A resolution. Science *292*, 1876–1882.

Hahn, S. (2004). Structure and mechanism of the RNA polymerase II transcription machinery. Nat. Struct. Mol. Biol. *11*, 394–403.

Hsieh, Y.J., Kundu, T.K., Wang, Z., Kovelman, R., and Roeder, R.G. (1999). The TFIIIC90 subunit of TFIIIC interacts with multiple components of the RNA polymerase III machinery and contains a histone-specific acetyltransferase activity. Mol. Cell. Biol. *19*, 7697–7704.

Hu, P., Wu, S., Sun, Y., Yuan, C.C., Kobayashi, R., Myers, M.P., and Hernandez, N. (2002). Characterization of human RNA polymerase III identifies orthologues for Saccharomyces cerevisiae RNA polymerase III subunits. Mol. Cell. Biol. *22*, 8044–8055.

Jones, T.A., Zou, J.Y., Cowan, S.W., and Kjeldgaard, M. (1991). Improved methods for building protein models in electron density maps and the location of errors in these models. Acta Crystallogr. *A47*, 110–119.

Kettenberger, H., Armache, K.-J., and Cramer, P. (2003). Architecture of the RNA polymerase II-TFIIS complex and implications for mRNA cleavage. Cell *114*, 347–357.

Kettenberger, H., Armache, K.-J., and Cramer, P. (2004). Complete RNA polymerase II elongation complex structure and its interactions with NTP and TFIIS. Mol. Cell *16*, 955–965.

Kettenberger, H., Eisenfuhr, A., Brueckner, F., Theis, M., Famulok, M., and Cramer, P. (2006). Structure of an RNA polymerase II-RNA inhibitor complex elucidates transcription regulation by noncoding RNAs. Nat. Struct. Mol. Biol. *13*, 44–48.

Landrieux, E., Alic, N., Ducrot, C., Acker, J., Riva, M., and Carles, C. (2006). A subcomplex of RNA polymerase III subunits involved in transcription termination and reinitiation. EMBO J. *25*, 118–128.

McCoy, A.J., Grosse-Kunstleve, R.W., Storoni, L.C., and Read, R.J. (2005). Likelihood-enhanced fast translation functions. Acta Crystallogr. D Biol. Crystallogr. *61*, 458–464.

Meinhart, A., Blobel, J., and Cramer, P. (2003). An extended winged helix domain in general transcription factor E/IIEalpha. J. Biol. Chem. *278*, 48267–48274.

Meka, H., Daoust, G., Arnvig, K.B., Werner, F., Brick, P., and Onesti, S. (2003). Structural and functional homology between the RNAP(I)

subunits A14/A43 and the archaeal RNAP subunits E/F. Nucleic Acids Res. *31*, 4391–4400.

Meka, H., Werner, F., Cordell, S.C., Onesti, S., and Brick, P. (2005). Crystal structure and RNA binding of the Rpb4/Rpb7 subunits of human RNA polymerase II. Nucleic Acids Res. *33*, 6435–6444.

Morozov, V., Mushegian, A.R., Koonin, E.V., and Bork, P. (1997). A putative nucleic acid-binding domain in Bloom's and Werner's syndrome helicases. Trends Biochem. Sci. *22*, 417–418.

Orlicky, S.M., Tran, P.T., Sayre, M.H., and Edwards, A.M. (2001). Dissociable Rpb4-Rpb7 subassembly of rna polymerase II binds to single- strand nucleic acid and mediates a post-recruitment step in transcription initiation. J. Biol. Chem. *276*, 10097–10102.

Otwinowski, Z., and Minor, W. (1996). Processing of X-ray diffraction data collected in oscillation mode. Methods Enzymol. *276*, 307–326.

Peyroche, G., Levillain, E., Siaut, M., Callebaut, I., Schultz, P., Sentenac, A., Riva, M., and Carles, C. (2002). The A14-A43 heterodimer subunit in yeast RNA pol I and their relationship to Rpb4-Rpb7 pol II subunits. Proc. Natl. Acad. Sci. USA *99*, 14670–14675.

Sadhale, P.P., and Woychik, N.A. (1994). C25, an essential RNA polymerase III subunit related to the RNA polymerase II subunit RPB7. Mol. Cell. Biol. *14*, 6164–6170.

Sakurai, H., Mitsuzawa, H., Kimura, M., and Ishihama, A. (1999). The Rpb4 subunit of fission yeast Schizosaccharomyces pombe RNA polymerase II is essential for cell viability and similar in structure to the corresponding subunits of higher eukaryotes. Mol. Cell. Biol. *19*, 7511–7518.

Schramm, L., and Hernandez, N. (2002). Recruitment of RNA polymerase III to its target promoters. Genes Dev. *16*, 2593–2620.

Schultz, P., Celia, H., Riva, M., Sentenac, A., and Oudet, P. (1993). Three-dimensional model of yeast RNA polymerase I determined by electron microscopy of two-dimensional crystals. EMBO J. *12*, 2601–2607.

Shpakovski, G.V., and Shematorova, E.K. (1999). Characterization of the rpa43+ cDNA of Schizosaccharomyces pombe: Structural similarity of subunit Rpa43 of RNA polymerase I and subunit Rpc25 of RNA polymerase III. Bioorg. Khim. *25*, 791–796.

Siaut, M., Zaros, C., Levivier, E., Ferri, M.L., Court, M., Werner, M., Callebaut, I., Thuriaux, P., Sentenac, A., and Conesa, C. (2003). An Rpb4/Rpb7-like complex in yeast RNA polymerase III contains the orthologue of mammalian CGRP-RCP. Mol. Cell. Biol. *23*, 195–205.

Terwilliger, T.C. (2002). Automated structure solution, density modification and model building. Acta Crystallogr. D Biol. Crystallogr. *58*, 1937–1940.

Thompson, J.D., Higgins, D.G., and Gibson, T.J. (1994). CLUSTAL W: improving the sensibility of progressive multiple sequence alignment through sequence weighing, positions-specific gap penalties and weight matrix choice. Nucleic Acids Res. *22*, 4673–4680.

Todone, F., Brick, P., Werner, F., Weinzierl, R.O., and Onesti, S. (2001). Structure of an archaeal homolog of the eukaryotic RNA polymerase II RPB4/RPB7 complex. Mol. Cell *8*, 1137–1143.

Ujvari, A., and Luse, D.S. (2006). RNA emerging from the active site of RNA polymerase II interacts with the Rpb7 subunit. Nat. Struct. Mol. Biol. *13*, 49–54.

Wang, Z., and Roeder, R.G. (1997). Three human RNA polymerase III-specific subunits form a subcomplex with a selective function in specific transcription initiation. Genes Dev. *11*, 1315–1326.

Weeks, C.M., and Miller, R. (1999). Optimizing Shake-and-Bake for proteins. Acta Crystallogr. D Biol. Crystallogr. *55*, 492–500.

Werner, M., Hermann-Le Denmat, S., Treich, I., Sentenac, A., and Thuriaux, P. (1992). Effect of mutations in a zinc-binding domain of yeast RNA polymerase C (III) on enzyme function and subunit association. Mol. Cell. Biol. *12*, 1087–1095.

Westover, K.D., Bushnell, D.A., and Kornberg, R.D. (2004a). Structural basis of transcription: nucleotide selection by rotation in the RNA polymerase II active center. Cell *119*, 481–489.

Westover, K.D., Bushnell, D.A., and Kornberg, R.D. (2004b). Structural basis of transcription: separation of RNA from DNA by RNA polymerase II. Science *303*, 1014–1016.

Zaros, C., and Thuriaux, P. (2005). Rpc25, a conserved RNA polymerase III subunit, is critical for transcription initiation. Mol. Microbiol. *55*, 104–114.

Accession Numbers

The Protein Data Bank accession number for the C17/25 subcomplex is 2ckz.